Electronic Supplemental Information

Appendix 1 The energy distribution between the confined diamond surfaces by L-J model

Here the L-J potential for atoms on each layer structures confined between parallel diamond surfaces is considered. As shown in Fig.1a, supposing that the first, second and third layers are chloride, carbon and chloride atoms respectively. The L-J potential interacting with two confined surfaces and surrounding particles is derived by superposition method. As L-J are short-range interaction and decreases fast with distance, the interactions between particle *P* and further layers are omitted. For example, particle *P* on surface S_{l1} will interact with two diamond surfaces and particles on the layer S_{l1} and S_{l2}, where the interactions with the particles in layers higher than S_{l3} are omitted. We use a unified power exponent function $U_{L-J}(r_{ij}) = C_n r^{-n}$ to express L-J potential for simplification, here $C_6 = -4\varepsilon\sigma^6$ for n=6 and $C_{12} = 4\varepsilon\sigma^{12}$ for n=12. The potential for each layer can be expressed as,

$$\begin{aligned} U_{P-on-S_{l1}} &= U_{P\text{-}S_1} + U_{P\text{-}S_2} + U_{P\text{-}S_{l1}} + U_{P\text{-}S_{l2}} \\ &= \frac{2\pi\rho_{S_1} C_{P\text{-}S_1}}{(n-2)(n-3)z^{n-3}} + \frac{2\pi\rho_{S_2} C_{P\text{-}S_2}}{(n-2)(n-3)(D-z)^{n-3}} \\ &\quad + \frac{2\pi\rho_{s_{l1}} C_{P\text{-}S_{l1}}}{(n-2)\tau_{S_{l1}}{}^{n-2}} + \frac{2\pi\rho_{s_{l2}} C_{P\text{-}S_{l2}}}{(n-2)h_{12}{}^{n-2}} \end{aligned} \tag{A1}$$

$$\begin{aligned} U_{P-on-S_{l2}} &= U_{P\text{-}S_1} + U_{P\text{-}S_2} + U_{P\text{-}S_{l1}} + U_{P\text{-}S_{l2}} + U_{P\text{-}S_{l3}} \\ &= \frac{2\pi\rho_{S_1} C_{P\text{-}S_1}}{(n-2)(n-3)z^{n-3}} + \frac{2\pi\rho_{S_2} C_{P\text{-}S_2}}{(n-2)(n-3)(D-z)^{n-3}} + \frac{2\pi\rho_{s_{l2}} C_{P\text{-}S_{l2}}}{(n-2)\tau_{S_{l2}}{}^{n-2}} \\ &\quad + \frac{2\pi\rho_{s_{l1}} C_{P\text{-}S_{l1}}}{(n-2)h_{12}{}^{n-2}} + \frac{2\pi\rho_{s_{l3}} C_{P\text{-}S_{l3}}}{(n-2)h_{23}{}^{n-2}} \end{aligned} \tag{A2}$$

$$\begin{aligned} U_{P-on-S_{l3}} &= U_{P\text{-}S_1} + U_{P\text{-}S_2} + U_{P\text{-}S_{l3}} + U_{P\text{-}S_{l2}} + U_{P\text{-}S_{l4}} \\ &= \frac{2\pi\rho_{S_1} C_{P\text{-}S_1}}{(n-2)(n-3)z^{n-3}} + \frac{2\pi\rho_{S_2} C_{P\text{-}S_2}}{(n-2)(n-3)(D-z)^{n-3}} \\ &\quad + \frac{2\pi\rho_{s_{l3}} C_{P\text{-}S_{l3}}}{(n-2)\tau_{S_{l3}}{}^{n-2}} + \frac{2\pi\rho_{s_{l2}} C_{P\text{-}S_{l2}}}{(n-2)h_{23}{}^{n-2}} + \frac{2\pi\rho_{s_{l4}} C_{P\text{-}S_{l4}}}{(n-2)h_{34}{}^{n-2}} \end{aligned} \tag{A3}$$

It is noted that the first two terms in Eqs. (A1, 2, 3) describe the interactions with two diamond surfaces, and the other terms are potential caused by surrounding particles. The ρ_{S_1} and ρ_{S_2} are the volume number density for both diamond substrates, $\rho_{S_{l1}}$, $\rho_{S_{l2}}$, $\rho_{S_{l3}}$, $\rho_{S_{l4}}$ are surface number density for each liquid layer, which is estimated by the bulk density of 1.584 g/cm3. The distance between each layer is derived as the equilibrium distance of $h = \sqrt[6]{2.5}\sigma$.

The equilibrium radius for particle on each surface is estimated by density based on hard sphere assumption. The Table S1 lists the values for specific parameters, C, τ, h The L-J interacting parameters are chosen from simulation OPLS-AA forcefield file, where for the carbon – carbon atoms interaction parameters with the substrates and the in the liquid are: $\varepsilon = 0.05\ kcal/mol$ and $\sigma = 3.8$ Å. For chlorine - chlorine atoms interaction in the liquid the parameters are: $\varepsilon = 0.266\ kcal/mol$ and $\sigma = 3.47$ Å. The carbon – chlorine atoms interaction in the liquid and between liquid/substrates are approximated with two parameters by mix geometric function in MD simulation, where $\varepsilon_{C-Cl} \approx \sqrt{\varepsilon_{C-C}\,\varepsilon_{Cl-Cl}} = 0.1153\ kcal/mol$ and $\sigma_{C-Cl} \approx \dfrac{(\sigma_{C-C} + \sigma_{Cl-Cl})}{2} = 3.635$ Å.

Table. S1. The parameters of L-J interaction potential for Eqs. (A1, 2, 3)

Parameter	ρ_{S_1} $\left(1/nm^3\right)$	ρ_{S_2} $\left(1/nm^3\right)$	$\rho_{S_{l1}}$ $\left(1/nm^2\right)$	$\rho_{S_{l2}}$ $\left(1/nm^2\right)$	$\rho_{S_{l3}}$ $\left(1/nm^2\right)$	$\rho_{S_{l4}}$ $\left(1/nm^2\right)$
Value	175.44	175.44	3.72	1.86	3.72	1.86
Layer atom	1 Cl(n=6)	2 C(n=6)	3 Cl(n=6)	1 Cl(n=12)	2 C(n=12)	3 Cl(n=12)
$C_{P\text{-}S_1}$ $\left(kcal\cdot nm^n/mol\right)$	1.064e-3	6.022e-4	1.064e-3	2.454e-6	1.813e-6	2.454e-6
$C_{P\text{-}S_2}$ $\left(kcal\cdot nm^n/mol\right)$	1.064e-3	6.022e-4	1.064e-3	2.454e-6	1.813e-6	2.454e-6
$C_{P\text{-}S_{l1}}$ $\left(kcal\cdot nm^n/mol\right)$	1.857e-3	1.064e-4	-	3.243e-6	1.813e-6	-
$C_{P\text{-}S_{l2}}$ $\left(kcal\cdot nm^n/mol\right)$	1.064e3	6.022e-4	1.064e-3	2.454e-6	2.454e-6	2.454e-6
$C_{P\text{-}S_{l3}}$ $\left(kcal\cdot nm^n/mol\right)$	-	1.064e-3	1.858e-3	-	2.454e-6	3.243e-6
$C_{P\text{-}S_{l4}}$ $\left(kcal\cdot nm^n/mol\right)$	-	-	1.858e-3	-	-	3.243e-6
$\tau_{S_{l1}}\left(nm\right)$	0.3895	-	-	0.3895	-	-
$\tau_{S_{l2}}\left(nm\right)$	-	0.4265	-	-	0.4265	-
$\tau_{S_{l3}}\left(nm\right)$	-	-	3.895	-	-	0.3895

$h_{12}\,(nm)$	0.4235	0.4235	-	0.4235	0.4235	-
$h_{23}\,(nm)$	-	0.4235	0.4235	-	0.4235	0.4235
$h_{34}\,(nm)$	-	-	0.4043	-	-	0.4043

Appendix 2 Simulation stability

The stability for the simulations has been tested by comparing the simulation runs for 50 ps, 200 ps and 1 ns for the case of Fig. 2b. The results are presented in Fig. S1. There is no remarkable discrepancy between the relative electron density profiles for the different simulation times as can be seen from the Fig S1c. Therefore, the rest of the simulations have been performed with run time of 50 ps.

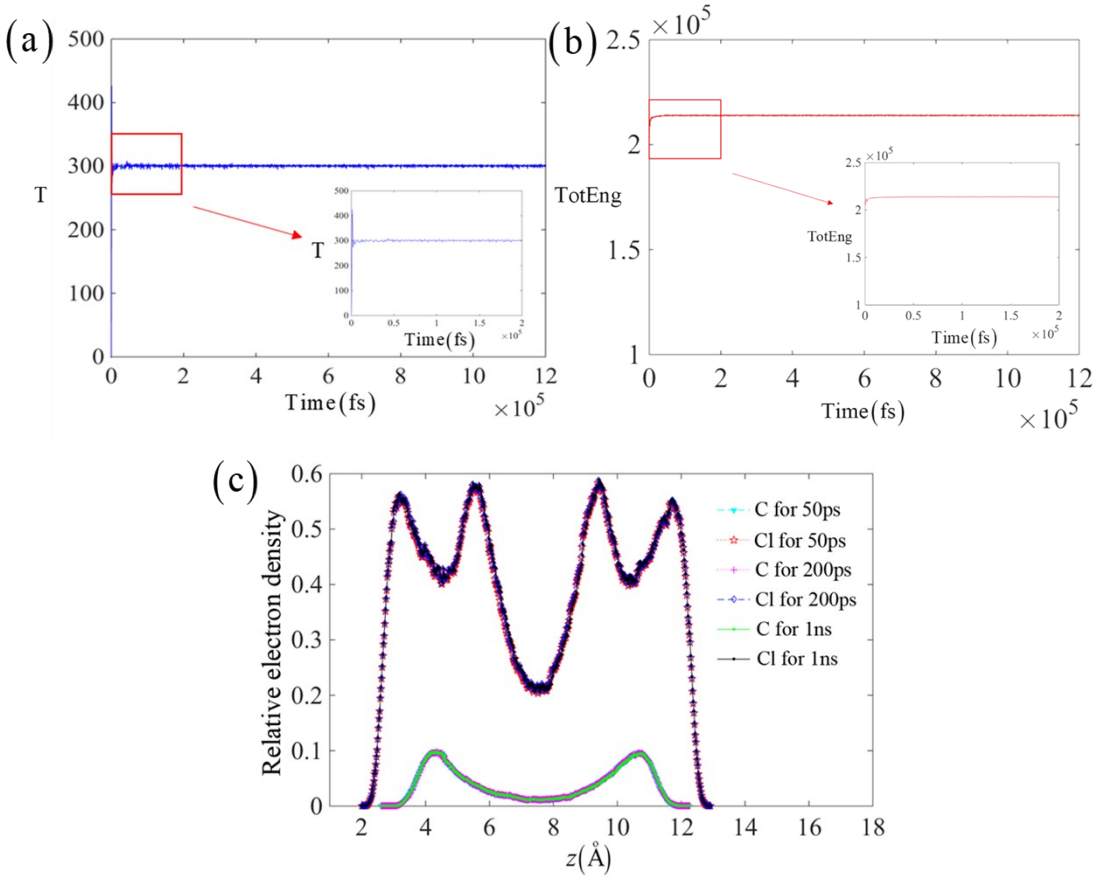

Fig. S1 (a) The temperature (in Kelvin) development during the simulation run; (b) The development of the total energy (TotEng); (c) The comparison between the relative electron density data for 50 ps, 200 ps and 1 ns.

Appendix 3 Simulation results with different gap size

The density profiles of CCl_4 films confined between two diamond surfaces with different gap size are calculated by using MD simulation (see Fig. S2). The simulation model is described in the main part. Here again, it is reminded, that the liquid density in the confined space is set to the bulk density. The compression process is simulated by decreasing the gap size (compression run), which leads to the increasing of the confined liquid density. In the following, the samples obtained thought compression run are compared with the samples where the simulation runs are performed at fixed gap (no compression) and bulk density. The simulations confirm that both cases lead to ordering of molecules in the gap. The orientational ordering and atomic layering for CCl_4 near the confined surface appear for larger gap size as well, even for samples with bulk density (Fig. S2 a, c, e, g). The comparison between Fig. S2 a, c, e, g with Fig. S2 b, d, f, h reveals that samples with higher density show slightly enhancement of the orientational ordering and atomic layering for the first layers near the surface While, the effect of confined surfaces is weak in the middle of the gap for both type of samples. The layering transition still exists but no molecular orientational is observed. In the middle of the gap the CCl_4 behave as spherical particles and the size of the layers is given by the size of the CCl_4 molecule.

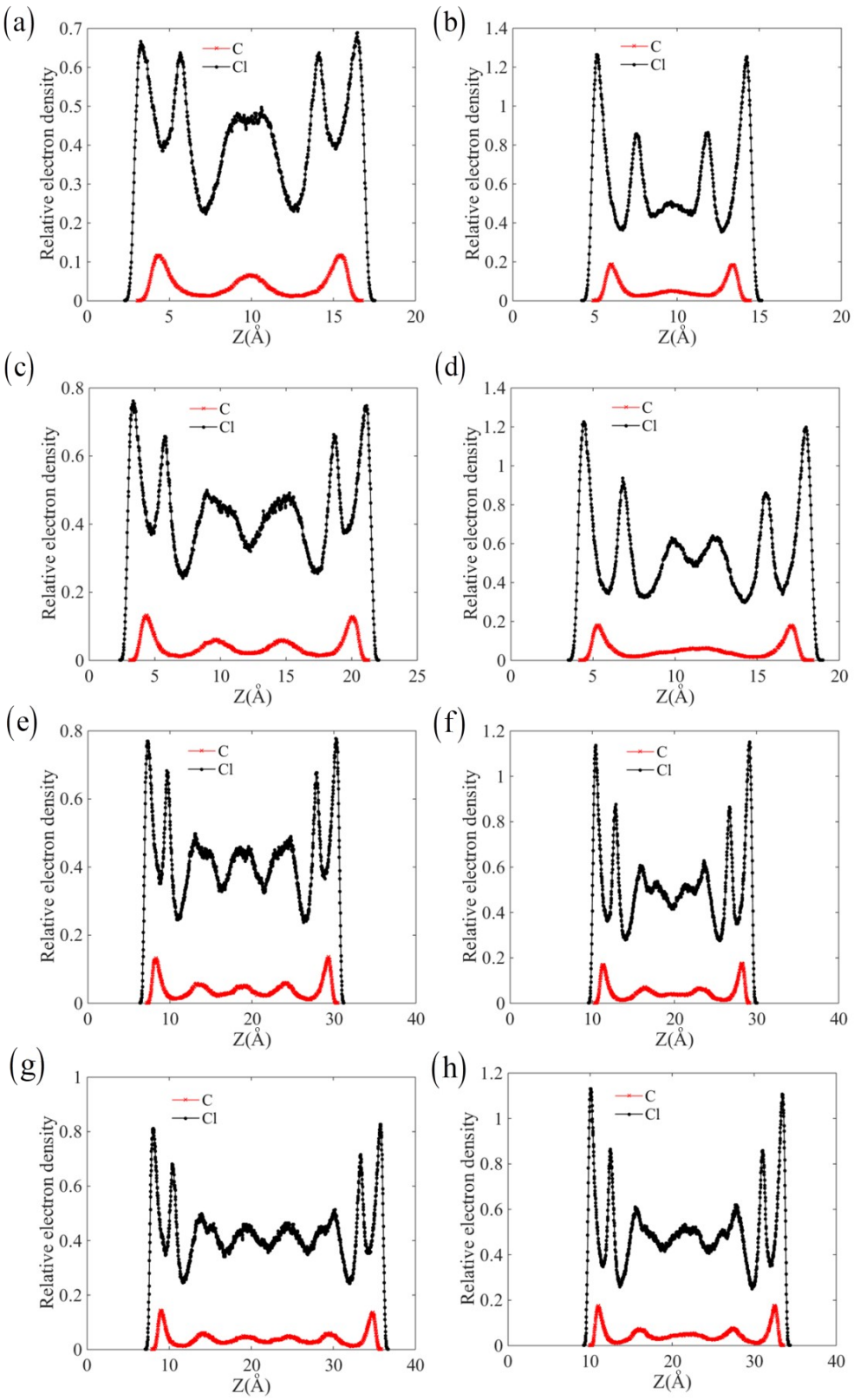

Fig. S2 The electric density profile for CCl_4 with different gap size: (a) gap size of 1.5nm with bulk density; (b) compression to ~1nm with initial gap size of 1.5nm; (c) gap size of 2nm with bulk density; (d) compression to ~1.5nm with initial gap size of 2nm; (e) gap size of 2.5nm with bulk density; (f) compression to ~2nm with initial gap size of 2.5nm; (g) gap size of 3nm with bulk density; (h) compression to ~2.5nm with initial gap size of 3nm.

Appendix 4 Electron density profile

The electron density profile calculated from the CCl_4 reflectivity curve describes the structure in the gap with two ordered molecular layers, which consists of two carbon and three chlorine sublayers and can be presented with the sequence: Cl+C+Cl+C+Cl. The oscillating density profile is imbedded in two buffer layers at the diamond surfaces. The layer interfaces are model with an error function and the total density profile is given by the sum of those layers (see equation 3 in the main part) with parameters presented in Table S2.

According to the nomenclature in [1] (see also Fig. S3), it could be distinguished nine different possible mutual orientations of the CCl_4 molecules in the two ordered molecular layers. In Table S3 are consider all possible stochiometric configurations of the chlorine atoms in the tree chlorine sublayers. In the following, the Theoretical Number Density Distribution (TNDD) of the chlorine atoms for each of those nine states is created. The TNDD is qualitatively compared with the total density profile calculated from the reflectivity data.

The TNDDs are calculated by a sum of three Gaussian distribution functions with certain position, width and scaling factor. The values for the position; p_1=0, p_2=2.83, p_3= p_2 + 2.9 and the widths; S_1 = 0.5, S_2 = 0.8, S_3 = 0.8 are derived from the values of 'thickness' and the 'roughness' in Table S2 for the corresponding chlorin layer. The scaling factors; C_1, C_{21}, C_{22}, C_3 are taken from Table S3 which gives the number of Cl atoms per layer and molecule for each of the nine cases. The factor **a**, **a** = $\rho_e S_{l2}$-C/$\rho_e S_{l4}$-C= 0.74 take in to account that $\rho_e S_{l2}$-C > $\rho_e S_{l4}$-C, in other words, in the second ordered C-layer (S_{l4}) there are less localized and structurally ordered molecules. Taking in to account the consideration above TNDDs can be calculated by:

$$TNDD = \frac{C_1}{\sqrt{2\pi {S_1}^2}}\exp\left(-\frac{x^2}{2{S_1}^2}\right) + \frac{C_{21}+aC_{22}}{\sqrt{2\pi {S_2}^2}}\exp\left(-\frac{(x-p_2)^2}{2{S_2}^2}\right) + \frac{aC_3}{\sqrt{2\pi {S_3}^2}}exp(-\frac{(x-p_3)^2}{2{S_3}^2}) \quad \text{(A4)}$$

Only three of the all nine TNDD profiles are similar to the electron density profile calculated form the reflectivity data, where the relation $\rho_e S_{l1}$-Cl > $\rho_e S_{l3}$-Cl > $\rho_e S_{l5}$-Cl is fulfilled. Those three TNDD profiles are represented in Fig. S4. According to this it follows that only corner-to-edge, corner-to-face and edge-to-edge profiles could correspond to the calculated X-ray density profile. In the corner-to-face the right peak (S_{l5}-Cl) is very week. In the edge-to-edge configuration the first peak (S_{l1}-Cl) is not well pronounced. Therefore, it is supposed that the

corner-to-face and edge-to-edge profiles also are not truly similar to the density profile obtained from the reflectivity data. The TNDD of the corner-to-edge configuration seems to be compatible to the density profile derived from the reflectivity data (see Fig.5b). This leads to the conclusion that the corner-to-edge configuration has higher probability in the molecular orientation distribution in the middle chlorine sublayer. This suggests that the confined space redefine the most probable mutual molecular configuration in comparison to the bulk. It is supposed that the confinement induces preferable orientation states between molecules and those states lead to localization of the C and Cl- atoms positions in sublayers.

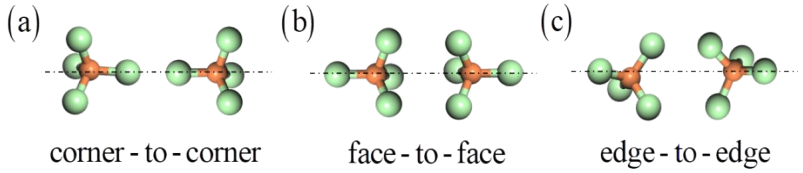

Fig. S3 The schematic drawing of different classes of configurations: (a) corner-to-corner (1:1); (b) face-to-face (3:3); (c) edge-to-edge (2:2).

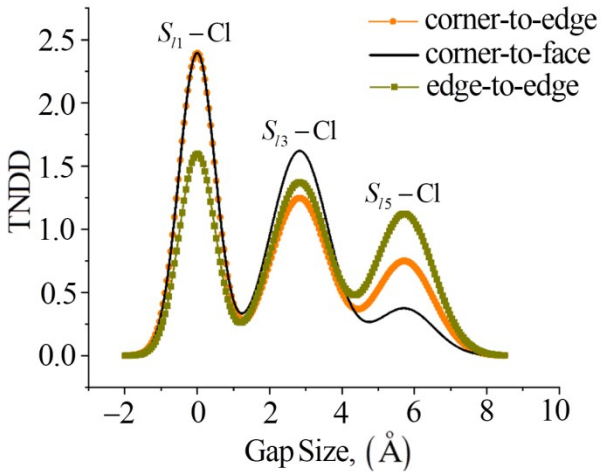

Fig. S4 The Theoretical number density distribution of the chlorin atoms per molecule in the gap for corner-to-edge (1:2) (orange); corner-to-face (1:3) (black); edge-to-edge (2:2) (dark yellow) configurations (see also Table S3).

Table S2. The parameter of the two buffer layers and the five liquid layers S_{l1}-Cl, S_{l2}-C, S_{l3}-Cl, S_{l4}-C and S_{l5}-Cl, calculated from the fitting of the reflectivity data.

	Thickness, [Å]	Roughness, [Å]	Dispersion x10^{-6}	ρ_e,x10^{24} [1/cm^3]

Substrate 1	-	6.0±0.5	2.24±0.01	1.06
Buffer layer 1	9.0±0.5	0.50 ±0.05	0.21±0.01	0.10
S_{l1}-Cl	1.35±0.01	0.52±0.05	1.53±0.01	0.72
S_{l2}-C	**1.35±0.01**	**0.70±0.05**	**0.83±0.01**	**0.39**
S_{l3}-Cl	1.62±0.01	0.80±0.05	0.86±0.01	0.41
S_{l4}-C	**1.34±0.01**	**0.56±0.05**	**0.61±0.01**	**0.29**
S_{l5}-Cl	1.50±0.01	0.80±0.05	0.75±0.01	0.35
Buffer layer 2	10.0±0.5	0.80±0.05	0.30±0.01	0.14
Substrate 2	-	7.0±0.5	2.24±0.01	1.06

Table S3. All possible configuration of Cl-atoms in both ordered molecular layers (notation after [1]). The theoretical number atom density of the Cl-atoms in S_{l3}-Cl-layer is a sum of the Cl-atoms per molecule from the first and the second ordered layer.

Configuration	Cl-atoms in S_{l1}-Cl-layer, C_1	Cl-atoms in S_{l3}-Cl-layer, C_{21} and C_{22}	Cl atoms in S_{l5}-Cl-layer, C_3
corner-to-face	3	1+3=4	1
corner-to-edge	3	1+2=3	2
corner-to-corner	3	1+1=2	3
edge-to-face	2	2+3=5	1
edge-to-edge	2	2+2=4	2
edge-to-corner	2	2+1=3	3
face-to-face	1	3+3=6	1
face-to-edge	1	3+2=5	2
face-to-corner	1	3+1=4	3

References

[1] R. Ray, *J. Chem. Phys.*, 2007, **126**, 164506.